HHS Public Access

Author manuscript

Virology. Author manuscript; available in PMC 2019 May 07.

Published in final edited form as:

Virology. 2018 June ; 519: 77–85. doi:10.1016/j.virol.2018.04.001.

Phosphorodiamidate morpholino targeting the 5′ untranslated region of the ZIKV RNA inhibits virus replication

Waldemar Popik[b], **Atanu Khatua**[b], **James E.K. Hildreth**[a,b], **Benjamin Lee**[c], and **Donald J. Alcendor**[a,*]

[a]Department of Microbiology and Immunology, Center for AIDS Health Disparities Research, Meharry Medical College, School of Medicine, 1005 Dr. D.B. Todd Jr. Blvd., Nashville, TN, 37208-3599, USA

[b]Department of Internal Medicine, Meharry Medical College, School of Medicine, 1005 Dr. D.B. Todd Jr. Blvd, Nashville, TN 37208-3599, USA

[c]Department of Obstetrics and Gynecology, Meharry Medical College, School of Medicine, 1005 Dr. D.B. Todd Jr. Blvd, Nashville, TN, 37208-3599, USA

Abstract

Background—Zika virus (ZIKV) infection has been associated with microcephaly in infants. Currently there is no treatment or vaccine. Here we explore the use of a morpholino oligonucleotide targeted to the 5′ untranslated region (5′-UTR) of the ZIKV RNA to prevent ZIKV replication.

Methods—Morpholino DWK-1 inhibition of ZIKV replication in human glomerular podocytes was examined by qRT-PCR, reduction in ZIKV genome copy number, western blot analysis, immunofluorescence and proinflammatory cytokine gene expression.

Results—Podocytes pretreated with DWK-1 showed reduced levels of both viral mRNA and ZIKV E protein expression compared to controls. We observed suppression in proinflammatory gene expression for IFN-β (interferon β) RANTES (regulated on activation, normal T cell expressed and secreted), MIP-lα (macrophage inflammatory protein-lα), TNF-α (tumor necrosis factor-α) and ILl-α (interleukin 1-α) in ZIKV-infected podocytes pretreated with DWK-1.

Conclusions—Morpholino DWK-1 targeting the ZIKV 5′-UTR effectively inhibits ZIKV replication and suppresses ZIKV-induced proinflammatory gene expression.

*Corresponding author. dalcendor@mmc.edu (D.J. Alcendor).

Author contributions

WP identified a morpholino target in ZIKV 5′-UTR. DJA and WP conceived and designed the study. WP, AK, DJA and BL performed the experiments. DJA, WP and JEKH drafted the manuscript. All authors read and approved the final version of the manuscript.

Publisher's Disclaimer: Disclaimer

Publisher's Disclaimer: The funders did not participate in the design, preparation, data analysis, or decision to publish the manuscript.

Potential conflicts of interest

The authors declare that they have no competing interests.

Keywords

Zika virus; Morpholino; Podocyte; Antiviral; Inflammation; Therapy

1. Introduction

Zika virus (ZIKV) is a member of the Flaviviridae family, genus Flavivirus, which also includes dengue virus, West Nile virus, Japanese encephalitis virus, and yellow fever virus (Faye et al., 2014; Hayes, 2009). ZIKV is a mosquito-borne arbovirus transmitted primarily by vectors from the Aedes family, in particular *Aedes aegypti* and *Aedes albopictus* (Vorou, 2016). ZIKV has quickly spread to more than 70 countries in the Americas and the Caribbean infecting more than 2 million people (Tappe et al., 2016; Center for Disease Control and Prevention, 2015; Center for Disease Control and Prevention, 2016). Infection with ZIKV results in asymptomatic disease in 70–80% of infected individuals, however ZIKV infection has been strongly associated with increased incidence of Guillain-Barre syndrome and microcephaly in infants. (Center for Disease Control and Prevention, 2015, Calvet et al., 2016; Adibi et al., 2016). Clinical presentations of ZIKV infection include skin rash, headache, myalgia, joint pain, and conjunctivitis but are largely self-limiting.

Currently there is no specific treatment or FDA approved vaccine for ZIKV infection. This represents an urgent unmet medical need for efficacious therapeutics for ZIKV. Vivo morpholinos have been shown to be effective at suppression of flavivirus replication in vitro and in vivo. Morpholino nucleotide oligomers are uncharged molecules that bind to cognate RNA sequences that can effectively block translation, inhibit miRNA maturation, or modify pre-mRNA splicing (Blum et al., 2015; Subbotina et al., 2016). The vivo-morpholino is composed of a morpholino oligo with a unique covalently linked delivery moiety, which is comprised of an octaguanidine dendrimer. The active component, namely the arginine rich delivery peptide of the guanidinium group facilitates delivery of the modified morpholino into the cytosol. Once introduced into cells morpholinos freely diffuse between cytoplasmic and nuclear compartments to effectively bind complementary RNA sequences. Morpholinos are soluble, have low-toxicity, stable at room temperature, and are currently in clinical trials.

Mukherjee et al., used a Retinoic acid inducible gene 1 (RIG 1) morpholino to suppress RIG-1 expression in a mouse model to understand neurogenesis caused by Japanese encephalitis virus (JEV) infection (Mukherjee, 2017). The RIG 1 morpholino showed a marked reduction in RIG I protein expression in mice after intracerebral injection. Nazmi et al., explored the effects of Toll-like receptor 7 (TLR7) induction of antiviral responses against single stranded RNA viruses in an animal model (Nazmi et al., 2014). They developed systemic and brain specific TLR7 knock-down mice (TLR7 KD) using vivo-morph-linos. They observed differences in susceptibility and survival of wild-type and systemic TLR7 (KD) mice to Japanese encephalitis virus (JEV) but no difference in susceptibility in brain-specific TLR7 (KD) animals. Both TLR7 KD showed reductions in antiviral response and increased viral loads in the brain. In addition, Nazmi et al., also showed that vivo-morpholinos against specific regions of 3′ or 5′ untranslated regions of Japanese encephalitis virus (JEV) genome resulted in increased survival and neuroprotection

in a challenged murine model of JEV (Nazmi et al., 2010). Anantpadma et al., demonstrated that peptide-conjugated phosphorodiamidate morpholino oligomers (PPMOs) directed against the JEV 3′ cyclization sequence (3′CSI) had significant antiviral activity in Vero cells and Neuro2A cells (Anantpadma et al., 2010). They also demonstrated 60–80% protection with the PPMO after lethal challenge in a mouse model with no detectable virus in brain tissue 2 days post infection. Zhang et al., demonstrated antiviral activity against West Nile virus (WNV) using PPMOs designed to interfere with the 5′CS/3′CSI or 5′UAR/3′UAR base pairings (Zhang et al., 2008). They showed that a single-nucleotide change within the 3′UAR-PPMO-target site conferred resistance to the PPMO. They have related this resistance to the blocking RNA/RNA interaction required for genome cyclization. Stein et al., has shown increased survival of AG129 mice infected with dengue 2 virus (DENV-2) after prior treatment with phosphor-odiamidate morpholino oligomers (PMO) and PPMO (Stein et al., 2008). Deas et al.; evaluated vivo efficacy of two PPMOs conjugated with an arginine-rich peptide against West Nile virus (WNV) (Deas et al., 2007). They observed antiviral activity against WNV, Japanese encephalitis virus, and St. Louis encephalitis virus by in vitro assays. Analysis of viruses resistant to PPMOs revealed the accumulation of mutation within the 5′ and outside the 3′ regions of the PPMO-target binding sites respectively. The designated PPMOs provided partial protection in animals and marginal toxicity at low doses.

Here we employ morpholino DWK-1 that is designed to bind to the ZIKV 5′-UTR RNA to block translation of the ZIKV polyprotein precursor (Harris et al., 2006). Here we utilize ZIKV-targeted vivo-morpholino to inhibit ZIKV replication. We demonstrate morpholino DWK-1 effectively inhibits ZIKV replication and suppresses ZIKV induced inflammatory gene expression in vitro in human glomerular podocytes and primary human retinal endothelial cells that we have identified as being highly permissive for ZIKV infection (Alcendor, 2017 and Roach, 2017). DWK-1 has unique features of a potential antiviral in humans that could be employed for ZIKV acute disease when ZIKV prophylaxis in the form of a vaccine is unwarranted as a treatment option.

2. Materials and methods

2.1. Morpholino oligomers

The ZIKV-targeted morpholino oligomer DWK-1 was designed to be complementary to the 25-mer nucleotide sequence within the ZIKV 5′ untranslated region (5′-UTR) (bolded in brackets) that includes the first ATG translation start codon (bolded, underlined) of the Zika virus strain PRVABC59 (GenBank mRNA transcript KU501215.1, PRVABC59/Puerto-Rico/2015):

5′GTATCAACAGGTTTTATTTTGGAT **[TTGGAAACGAGAGTTTCTG GTC<u>AUG</u>]**AAAAACC

CAAAAAAGAAATCCG-3′. The 5′-UTR of the ZIKV PRVABC59 RNA sequence targeted by DWK-1 is highly conserved among ZIKV strains. The sequence of DWK-1 complementary to the 25-mer of ZIKV 5′-UTR is as follows: 5′-CATGACCAGAAACTCTCGTTTCCAA-3′. The control oligo used in this study is a

standard control oligo that targets a human beta-globin intron mutation that causes beta-thalassemia. This oligo, designated as Co DWK-1, causes little change in phenotype in any known test system except human beta-thalessemic hematopoetic cells and is appropriate negative control for custom vivo-morpholino oligos (Moulton, 2017). The sequence of Co DWK-1 is as follows: 5′-CCTCTTACCTCAGTTACAATTTATA-3′. Morpholino oligonucleotides used in all experiments (vivo-morpholinos) were conjugated to a delivery moiety consisting of an eight-branched dendrimer carrying a guanidinium moiety at each branch tip (see Fig. 1) for efficient delivery of morpholino to the cytosol and nuclear compartments of the cell. The vivo-morpholinos DWK-1 and Co DWK-1 were synthesized by Gene Tools, LLC. The rationale for using 25-mers which is the longest commercially available morpholino is that they are recommended for most applications. This is because efficacies increase substantially with increasing length and because long oligos best assure access to a single-stranded region in the target RNA, as is required for nucleation of pairing by the oligo (Summerton and Weller,1997; Heasman 2002). This length versus activity study was carried out by Gene Tools with morpholino oligos and 25 mers were found to be the optimal length for sequence specific knockdown of genes in mammalian cells.

2.2. Cells

Immortalized human glomerular podocytes AB8/13 were obtained from Moin A. Saleem (Saleem et al., 2002) and were cultured as described (Khatua et al., 2010). Cells were trypsinized and plated in 6 well dishes at a concentration 3.5×10^5 per well. The cells were cultured in RPMI media supplemented with 10% FCS and insulin-transferrin-selenium (ITS; ThermoFisher Scientific).

2.3. Morpholino pretreatment

Lyophilized morpholino oligos DWK-1 and Co-DWK-1 were dissolved in sterile water to a final concentration of 0.5 mM. A 30 μl aliquot was added to podocytes cultured in fresh 1.5 ml RPMI media supplemented with 10% FCS and ITS per well of 6-well dishes. The final concentration of DWK-1 and Co DWK-1 in culture medium was 10 μM. After 24 h incubation, podocytes were rinsed with culture medium and either mock infected or infected with ZIKV and cultured for the indicated time in the absence of morpholinos.

2.4. Cytotoxicity assay for in vivo-morpholino

AB813 cells were seeded in triplicate in 96-well plate at 15,000 cells/well/100 μl. Next day, media were replaced with fresh 100 μl RPMI 10% FCS supplemented with ITS and different concentrations of DWK-1 were added. The cells were incubated for 24 h followed by the addition of 20 μl of Component A (Cell cytotoxicity assay kit, Abcam # ab112118) and incubation for 3h at 37 °C, according to the manufacturer protocol. The absorbance intensity was measured at 570 nm and 605 nm. The percentage of cell viability for different concentrations of tested compound (DWK-1), non-cell control (media only) and cells without added DWK-1 was calculated according to the formula: % Cell viability = $100 \times [(\text{Rsample} - R_0)/(\text{Rctrl} - R_o)]$, where Rsample is the absorbance ratio of $OD_{570}/OD_{60}5$ for DWK-1, Rctrl is the OD_{570}/OD_{605} ratio in the absence of DWK-1 and R_0 is the averaged background absorbance ratio of OD_{570}/OD_{605} for media only (non-cell control).

2.5. ZIKV preparation and titration

The Zika virus strain PRVABC59 used in this study was originally isolated from a human serum specimen from Puerto Rico in December 2015, nucleotide (GenBank): KU501215 ZIKV strain PRVABC59, complete genome (Lanciotti et al., 2015; Thomas et al., 2016; Dirlikov et al., 2016; Lanciotti et al., 2008). The virus was cultivated in Vero cells and infectious supernatant was filtered using a 0.22 μm filter and the serum content adjusted to 15%. Stock viral titers were determined as previously described (Alcendor, 2017). All experiments were carried out under biosafety level-2 containment as recommended. Use of ZIKV was approved by the Meharry Medical College Institutional Review Board and the Institutional Biosafety Committee.

2.6. ZIKV RNA analysis

Total cellular RNA was isolated from the cells using Quick RNA MiniPrep kit (Zymo Research) and 500 ng RNA was reverse transcribed into cDNA using iScript cDNA synthesis kit (Bio-Rad). Real-time PCR was performed on CFX96 PCR machine (Bio-Rad) using SYBR Green PCR master mix (Bio-Rad), ZIKA specific primers (forward primer 5′-CCGCTGCCCAACACAAG-3′ and reverse primer 5′-CCACTAACGTTC TTTTGCAGACAT-3′) and GAPDH specific primers (forward 5′-GAAGG TGAAGGTCGGAGT-3′ and reverse 5′-GAAGATGGTGATGGGATTTC-3′). The following amplification conditions were used: 95 °C for 3 min for initial denaturation and 40 cycles of 95 °C for 10 s and 60 °C for 45 s. Samples were analyzed in triplicate and ZIKV RNA expression was normalized to GAPDH mRNA levels. Data are presented as mean ± SD. A standard curve was generated by using the 10-fold serial dilutions of a synthetic ZIKV RNA (ATCC VR-3252SD) with known ZIKV genome copies (provided as 1.2×10^6 copies/μl). Absolute quantification of ZIKV genome copy numbers was carried out in triplicate by comparing each sample′s threshold cycle (C_T) value with a ZIKV RNA standard curve.

2.7. qRT-PCR analysis of the proinflammatory cytokine gene expression

Total cellular RNA was isolated, processed and analyzed as described above. The primers used to analyze cytokine gene expression are as follows: IFN-β: forward

5′-CTTGGATTCCTACAAAGAAGCAGC-3′, reverse 5′-TCCTCCTTCT GGAAC TGCTGCA-3′; RANTES: forward 5′-CCTGCTGCTTTGCCTACAT TGC-3′, reverse 5′-ACACACTTGGCGGTTCTTTCGG-3′; MIP-lα: forward 5′-ACTTTGAGACGAGCAGCCAGTG-3′, reverse 5′-TTTCTGGACCCACTC CTCACTG-3′; TNF-α: forward S′-CTCTTCTGCCTGCTGCACTTTG-3′, reverse 5′-ATGGGCTACAGGCTTGTCACTC-3′; IL-lα: forward 5′-TGTAT GTGACTGCCCAAG ATGAAG-3′, reverse 5′-AGAGGAGGTTGGTCTCAC TACC-3′; IL-6: forward 5′-AGACAGCCA CTCACCTCTTCAG-3′, reverse 5′-TTCTGCCAGTGCCTCTTTGCTG-3′.

Samples were analyzed in triplicate and cytokine gene expression was normalized to GAPDH mRNA levels.

2.8. Immunofluorescence

Immunofluorescent staining was performed as previously described (Alcendor, 2017). Briefly, chamber slide cultures containing mock infected human podocytes, podocytes infected with ZIKV and podocytes infected ZIKV after 24 h pre-treatment with DWK-1. Cells were washed twice with PBS pH 7.4, air dried, and fixed in absolute methanol for 20 min at – 20 °C. Cells were air dried for 10 min, hydrated in Tris buffered saline (pH 7.6) for 10 min, and incubated for 1 h with the 4G-2 Flavivirus group antigen monoclonal antibodies from Millipore (Temecula, CA, USA) at a dilution 1:100 in PBS pH 7.4. (Wilkerson et al., 2015).

2.9. Western blot analysis

Cell extracts were prepared using RIPA lysis buffer [50 mM Tris pH 7.5, 150 mM NaCl, 2 mM ethylenediaminetetraacetic acid (EDTA) pH 8.0, 1% NP40, 0.5% sodium deoxycholate, 0.1% sodium dodecyl sulfate (SDS), and proteinase inhibitor (Complete Ultra, Roche). Lysates were incubated on ice for 30 min and then clarified by centrifugation. Total protein was measured by micro BCA protein assay kit (ThermoFisher Scientific). Protein lysates (30 μg) were separated by 10% SDS-PAGE, transferred to nitrocellulose membranes (Bio-Rad), blocked with 5% milk in 0.1% TBST (0.1% Tween 20, 20 mM Tris, 150 mM NaCl) and incubated at 4 °C overnight with 4 G-2 Flavivirus group antigen monoclonal antibody (Millipore, Temecula, CA, USA) at 1:250 dilution. Synaptopodin antibody (Santa Cruz Biotechnology) was used at 1:250 dilution and GAPDH antibody (Santa Cruz Biotechnology) at 1:3000 dilution. Membranes were washed five times in 0.1% TBST and incubated for one hour with corresponding secondary antibody conjugated with HRP (ThermoFisher Scientific) at a dilution of 1:50,000. Immunoreactive bands were detected with WesternBright ECL (Advansta) following exposure to X-ray film.

2.10. Statistical analysis

Experiments presented in this study were performed independently three times under similar conditions. Data are presented as means with standard deviations. Unpaired *t*-test was used to compare the mean values between groups. Differences were considered statistically significant at $P < 0.05$.

3. Results

3.1. DWK-1 inhibits accumulation of intracellular ZIKV RNA in a dose-dependent manner

To determine an effective concentration of vivo-morpholino DWK-1 (Fig. 1) that inhibits ZIKV replication in human podocytes, the cells were pretreated for 24 h with various concentrations of DWK-1 and Co DWK-1 ranging from 1 to 10 μM, rinsed and mock infected or infected with ZIKV (PRVABC59) at a multiplicity of infection (MOI) of 0.1 in the absence of morpholinos. In addition, human podocytes showed no significant cytotoxic effects after 24 h exposure to DWK-1 from 1.0 to 10 μM (Fig. 2). To determine ZIKV RNA accumulation in podocytes, cells were infected for 72 h collected and intracellular ZIKV RNA was determined by qRT-PCR (Fig. 3). Results show that DWK-1 reduced intracellular ZIKV RNA accumulation in a dose-dependent concentration with ~50% inhibition of ZIKV

RNA accumulation at 1.0–1.5 μM and > 95% inhibition at 10 μM. In contrast, Co-DWK-1 shows only a small inhibition (9 ± 5%) at 10 μM. Since 10 μM concentration of DWK-1 was of low toxicity to the cells, it was used in all experiments.

3.2. DWK-1 suppression of ZIKV progeny released from infected podocytes

To evaluate the effects of DWK-1 inhibition on progeny virus released from ZIKV infected podocytes, we examined the infectivity of supernatants from mock infected podocytes, podocytes exposed to the control morpholino only, podocytes exposed to DWK-1 only, ZIKV infected podocytes as well as infected podocytes treated with the control morpholino and infected podocytes treated with DWK-1 (Fig. 4A). First, we determined the level of DWK-1 inhibition of ZIKV transcription in podocytes (Fig. 4A). We consistently observed a > 96% inhibition of ZIKV transcription in infected podocytes treated with DWK-1 compared to ZIKV infection alone (Fig. 4A). There was no detectable ZIKV transcription in uninfected controls cells (Fig. 4A). Then, ten microliters of supernatant from the cultures shown in Fig. 4A were added to fresh podocyte and qRT-PCR was performed to determine if DWK-1 treatment would inhibit ZIKV progeny released from infected cell (Fig. 4B). Here we show a 97% reduction in infectivity of progeny virus released in supernatant from ZIKV infected podocytes treated with DWK-1 compared to controls (Fig. 4B). Another ten microliters of supernatant from cultures in Fig. 4A was added to fresh podocytes in four well chamber slides to determine progeny virus infectivity by a fluorescent focus assay (Fig. 4C). Here we observed an average of 81 +/−12 cells staining positive for ZIKV infected podocytes treated with DWK-1 (Figs. 4C–6) compared to 2782 +/−326 cells staining positive in ZIKV infected cells without treatment with DWK-1 (Figs. 4C–4). We also observed 2117 +/−274 ZIKV positive cells among podocytes treated with the control morpholino (Figs. 4C–5). There was no detectable ZIKV positive cells in uninfected controls cells (Figs. 4C–1–2 and 3).

3.3. DWK-1 suppression of ZIKV infectivity in primary human retinal endothelial cells

To evaluate the effects of DWK-1 of ZIKV infectivity in primary cells relevant to ZIKV pathogenesis in humans, we examined primary human retinal endothelial cells for inhibition of on ZIKV transcription by DWK-1 using qRT-PCR (Fig. 5). We observed a 98% reduction in ZIKV transcription in infected retinal endothelial cells exposed to DWK-1 (Fig. 5). We also observed no detectable amplification of ZIKV transcripts in mock infected or cells treated with both the control morpholino and DWK-1 alone (Fig. 5). We observed a lower level of ZIKV transcriptional amplification in ZIKV infected cells exposed to the control morpholino (Fig. 5).

3.4. DWK-1 reduces expression of intracellular ZIKV RNA in podocytes

To validate further the antiviral activity of DWK-1, we measured ZIKV RNA copy number in infected podocytes or podocytes pretreated with DWK-1 or Co DWK-1 and subsequently infected with ZIKV. First, we generated a standard curve by using 10-fold dilutions of synthetic ZIKV RNA (ATCC VR-3252SD) (Fig. 6A). The standard curve covered a linear range from 10^6 to 10 copies of ZIKV RNA with a slope = −3.923 and R^2 = 0.997, indicating a good sensitivity of the SYBR Green qRT-PCR assay (Fig. 6B). Total cellular RNA was isolated from podocytes treated as indicated in Fig. 6C and analyzed by qRT-PCR for the

expression of ZIKV and GAPDH transcripts. Results demonstrate 95% reduction of ZIKV RNA expression in podocytes pretreated with DWK-1 and infected for 48 h with ZIKV, as compared to infected podocytes pretreated with Co DWK-1. These results correlate with ~94% reduction of ZIKV RNA copy number (Fig. 6D) as quantitated from a standard curve (Fig. 6B) generated using synthetic ZIKV RNA.

3.5. DWK-1 strongly reduces expression of ZIKV E protein in infected podocytes

To determine if DWK-1 inhibition of ZIKV transcription in infected human glomerular podocytes results in a decrease in ZIKV protein expression, we examined expression of ZIKV E protein in podocytes pretreated with DWK-1. Immunofluorescent staining shows that E protein-specific 4 G-2 antibody does not stain mock infected podocytes, while podocytes infected with ZIKV for 72 h show characteristic perinuclear staining with the 4 G-2 antibody (Figs. 7A–1 and 7A–2). In contrast, podocytes pretreated with DWK-1 and infected with ZIKV for 72 h show only a minimal, if any, expression of ZIKV E protein as compared to mock and isotype controls (Figs. 7A–3 and 7A–4).

Similarly, expression of ZIKV E protein in infected podocytes after pretreatment with DWK-1 (ZIKV + DWK-1) was strongly reduced (> 98%) by immunoblot analysis (Fig. 7B). We observed no E protein expression in uninfected (Mock, Co DWK-1, DWK-1) podocytes. We also demonstrated that expression of the podocyte biomarker Synaptopodin was not significantly affected by ZIKV infection or podocyte exposure to DWK-1 or Co DWK-1 (Fig. 7B).

3.6. DWK-1 inhibits ZIKV-induced proinflammatory gene expression in podocytes

ZIKV virus infection leads to the induction of proinflammatory cytokines (Tappe et al., 2016; Maharajan et al., 2016). We examined whether DWK-1 pretreatment affects expression of proinflammatory cytokine genes in ZIKV infected podocytes (Fig. 8). Strikingly, ZIKV induced a robust 4023-fold increase in IFN-β gene expression and 3330-fold increase in podocytes pretreated with Co DWK-1 (Fig. 8A), when compared to mock infected cells. Importantly, pretreatment with DWK-1 prior to ZIKV infection resulted in over a 16-fold suppression of IFN-β transcriptional expression, as compared to cells pretreated with Co DWK-1 (Fig. 8A). Similarly, we observed a strong upregulation of RANTES transcriptional expression at 72 h after infection with ZIKV (58.8-fold increase) and in cells pretreated with Co DWK-1 and infected with ZIKV (47.2-fold increase) (Fig. 8B). Pretreatment of podocytes with DWK-1 prior to ZIKV infection resulted in > 9-fold reduction in RANTES gene expression, when compared to levels detected in infected podocytes pretreated with Co DWK-1 (Fig. 8B). No significant changes in the RANTES transcriptional expression were observed in mock podocytes or podocytes exposed to the DWK-1 or Co DWK-1 alone (Fig. 8B). Although the expression of MIP-1 α, TNF-α and IL-Iα was not so potently induced by ZIKV in podocytes (~2–4-fold upregulation) when compared to IFNβ or RANTES, pretreatment with DWK-1 prior to ZIKV infection reduced expression of these genes to levels detected in mock infected podocytes (Fig. 8C–E). No significant changes in IL-6 transcriptional expression were detected in podocytes exposed to DWK-1 prior to ZIKV infection, when compared to infected podocytes preexposed to Co DWK-1 (Fig. 8F).

4. Discussion

In this study, we demonstrate the effectiveness of the ZIKV targeted morpholino DWK-1 to suppress active transcription of ZIKV in vitro by approximately 95% and to reduce ZIKV E protein expression to undetectable levels. We show low level cytotoxicity in podocytes exposed to DWK-1 (Fig. 2). Using qRT-PCR and fluorescent focus assay, we demonstrate DWK-1 suppression of ZIKV infectious progeny in vitro by > 95% (Fig. 4). We also demonstrate strong inhibition of ZIKV transcription by the DWK-1 morpholino in primary human retinal endothelial cells (Fig. 5). In addition, we show that DWK-1 has no effect on the steady state expression levels of the podocyte specific biomarker synaptopodin. We also show that DWK-1 potently reduced expression of IFN-β, RANTES, MIP-1α and TNF-α in ZIKV infected cells, as compared to infected cells pretreated with Co DWK-1.

Zika virus has become a global threat that has spread to more than 80 countries around the world and the incidence of infection is increasing in the general population. The level of asymptomatic ZIKV infections are unknown and it is essential to control sporadic outbreaks of ZIKV infection in a timely manner. Currently there is no specific treatment or vaccine for ZIKV infection. The estimated number of pregnant women with evidence of ZIKV infection is increasing daily and the future impact on the health care systems around the world will be significant.

Once a ZIKV vaccine is approved, antivirals would complement a vaccine as a part of comprehensive strategy to curtail or prevent sporadic outbreaks and associated ZIKV pathologies. Morpholino based antivirals have the potential to be highly useful as prophylaxis or treatment for immunosuppressed SOTp receiving allografts from ZIKV infected donors as well as an anti-infective for protecting a blood supply tainted with ZIKV especially in ZIKV endemic regions where ZIKV screening of blood is unavailable.

Antivirals designed to inhibit active replication of ZIKV would be beneficial for these patients and could potentially suppress sporadic outbreaks of ZIKV infection in the general population. Such an antiviral that is stable at room temperature could be highly useful in arid conditions without refrigeration. This advantage could also enable development of a carry-on intervention to prevent ZIKV infection for military personnel and humanitarian workers traveling to ZIKV endemic regions.

5. Conclusions

We have designed a morpholino-based antiviral that targets ZIKV 5-′-UTR, is of low-toxicity, stable at room temperature and can penetrate target cells. DWK-1 belongs to a family of morpholino compounds known to be long acting in vivo, scalable, clinically applicable, and can be configured to cross cellular barriers. DWK-1 is a novel antiviral that effectively inhibits ZIKV replication, protein expression, and suppresses ZIKV induced inflammatory gene expression in vitro. DWK-1 has unique features that make it a potentially highly effective antiviral for ZIKV. Next steps in exploring this potential will be to examine in vivo toxicity and demonstrate DWK-1 inhibition of ZIKV in an animal model of acute ZIKV disease.

Acknowledgements

DJA and WP were supported by a Zika Virus Research Startup Award from the Meharry Medical College. WP and DJA made equal contributions to this manuscript.

References

Adibi JJ, Zhao Y, Cartus AR, Gupta P, Davidson LA, 2016 Placental mechanics in the Zika-microcephaly relationship. Cell Host Microbe 1, 9–11.

Alcendor DJ, 2017 Zika Virus infection of the human glomerular cells: implications for viral reservoirs and renal pathogenesis. J. Infect. Dis 171 10.1093/infdis/jixl71. [PubMed: 28073857]

Anantpadma M, Stein DA, Vrati S„, 2010 Inhibition of Japanese encephalitis virus replication in cultured cells and mice by a peptide-conjugated morpholino oligomer. J. Antimicrob. Chemother 5, 953–961.

Blum M, De Robertis EM, Wallingford JB3, et al., 2015 Morpholinos: antisense and sensibility. Dev. Cell 2, 145–149.

Calvet G, Aguiar RS, Melo AS, et al., 2016 Detection and sequencing of Zika virus from amniotic fluid of fetuses with microcephaly in Brazil: a case study. Lancet Infect. Dis 6, 653–660.

Centers for Disease Control and Prevention. CDC Newsroom. First case of Zika virus reported in Puerto Rico. <http://www.cdc.gov/media/releases/2015/sl231-zika.html>.

Centers for Disease Control and Prevention, 2016 Zika Travel Information; Zika Virus in the Caribbean, <http://wwwnc.cdc.gov/travel/notices/alert/zika-virus-caribbean>.

Deas TS, Bennett CJ, Jones SA, et al., 2007 In vitro resistance selection and in vivo efficacy of morpholino oligomers against West Nile virus. Antimicrob. Agents Chemother. 7, 2470–2482.

Dirlikov E, Ryff KR, Torres-Aponte J.et al. 2016 Update: Ongoing Zika Virus Transmission-Puerto Rico, November 1, 2015-April 14 MMWR Morb Mortal Wkly Rep 2016; 17:451–55.

Faye O, Freire CCM, Iamarino A, et al., 2014 Molecular evolution of Zika virus during its emergence in the 20th century. PLoS Negl. Trop. Dis. 8, e2636. [PubMed: 24421913]

Harris E, Holden KL, Edgil D, et al. Molecular biology of flaviviruses.Novartis Found Symp 2006; 277:23–39; discussion 40, 71–3, 251–3. [PubMed: 17319152]

Hayes EB, 2009 Zika virus outside Africa. Emerg. Infect. Dis 15, 1347–1350. [PubMed: 19788800]

Heasman J, 2002 Morpholino oligos: making sense of antisense? Dev. Biol 2, 209–214.

Khatua AK, Taylor HE, Hildreth JE, et al., 2010 Non-productive HIV-1 infection of human glomerular and urinary podocytes. Virology 1, 119–127.

Lanciotti RS, Kosoy OL, Laven, et al., 2008 Genetic and serologic properties of Zika virus associated with an epidemic, Yap State, Micronesia, 2007. Emerg. Infect. Dis 14, 1232–1239. [PubMed: 18680646]

Maharajan MK, Ranjan A, Chu JF, et al., 2016 Zika Virus nfection: current concerns and perspectives. Clin. Rev. Allerg. Immunol, 10.1007/sl2016-016-8554-7.

Mukherjee S, Ghosh S, Nazmi A, et al., 2015 RIG-I knockdown impedes neurogenesis in a murine model of Japanese encephalitis. Cell Biol. Int 2, 224–229.

Moulton JD, 2017 Using morpholinos to control gene expression. Curr. Protoc. Nucleic Acid. Chem 68, 430 (1–4.30.29). [PubMed: 28252184]

Nazmi A, Dutta K, Basu A, 2010 Antiviral and neuroprotective role of octaguanidinium dendrimer-conjugated morpholino oligomers in Japanese encephalitis. PLoS Negl. Trop. Dis 11, e892.

Nazmi A, Mukherjee S, Kundu K, et al., 2014 TLR7 is a key regulator of innate immunity against Japanese encephalitis virus infection. Neurobiol. Dis 69, 235–247. [PubMed: 24909816]

Roach T, Alcendor DJ, 2017 Zika Virus Infection of retinal endothelial cells: implications for viral associated congenital ocular disease. J. Neuroinflamm 14, 43.

Stein DA, Huang CY, Silengo S, et al., 2008 Treatment of AG129 mice with antisense morpholino oligomers increases survival time following challenge with dengue 2 virus. J. Antimicrob. Chemother 3, 555–565.

Subbotina E, Koganti SR, Hodgson-Zingman DM, et al., 2016 Morpholino-driven gene editing: a new horizon for disease treatment and prevention. Clin. Pharmacol. Ther 1, 21–25.

Summerton J, Weller D, 1997 Morpholino antisense oligomers: design, preparation, and properties. Antisense Nucleic Acid. Drug Dev 3, 187–195.

Tappe D, Pérez-Girón JV, Zammarchi L, et al., 2016 Cytokine kinetics of Zika virus-infected patients from acute to reconvalescent phase. Med. Microbiol. Immunol 3, 269–273.

Thomas DL, et al., Sharp TM, Torres J, 2016 Local transmission of Zika Virus - Puerto Rico. MMWR Morb. Mortal. Wkly. Rep. 6, 154–158 November 23, 2015-January 28.

Vorou R1, 2016 Zika virus, vectors, reservoirs, amplifying hosts, and their potential to spread worldwide: what we know and what we should investigate urgently. Int. J. Infect. Dis S1201–9712 (16), 31057–31058.

Wilkerson I, Laban J, Mitchell JM, et al., 2015 Retinal pericytes and cytomegalovirus infectivity: implications for HCMV-induced retinopathy and congenital ocular disease. J. Neuroinflamm 12, 2.

Zhang B, Dong H, Stein DA, Shi PY, 2008 Co-selection of West Nile virus nucleotides thatconfer resistance to an antisense oligomer while maintaining long-distance RNA/RNA basepairings. Virology 1, 98–106.

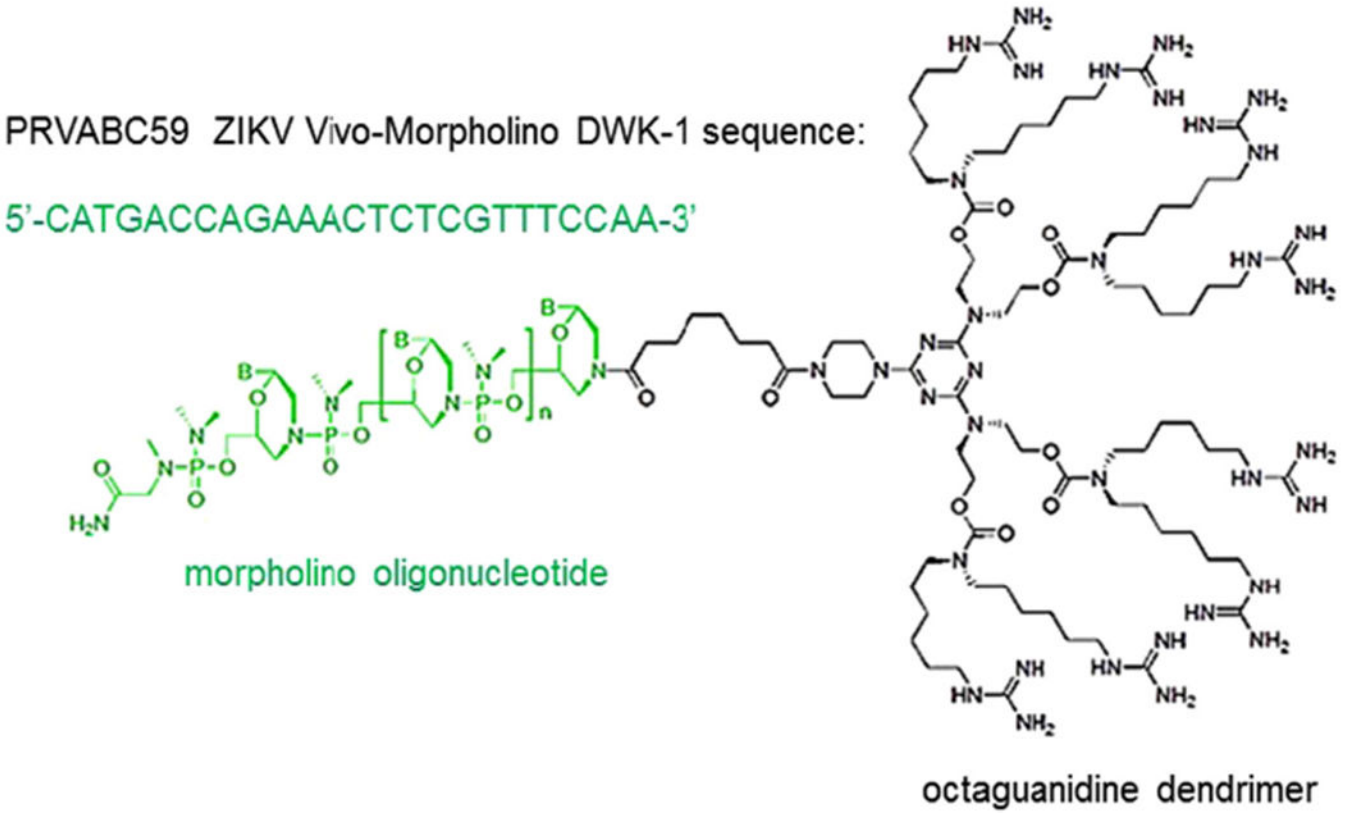

Fig. 1.

Schematic structure of a vivo-morpholino. A vivo-morpholino is composed of a 25-mer long morpholino oligonucleotide (green) covalently linked to an octaguanidine dendrimer (black), which serves as a delivery moiety. A nucleotide sequence of ZIKV PRVABC59 vivo-morpholino DWK-1 is shown.

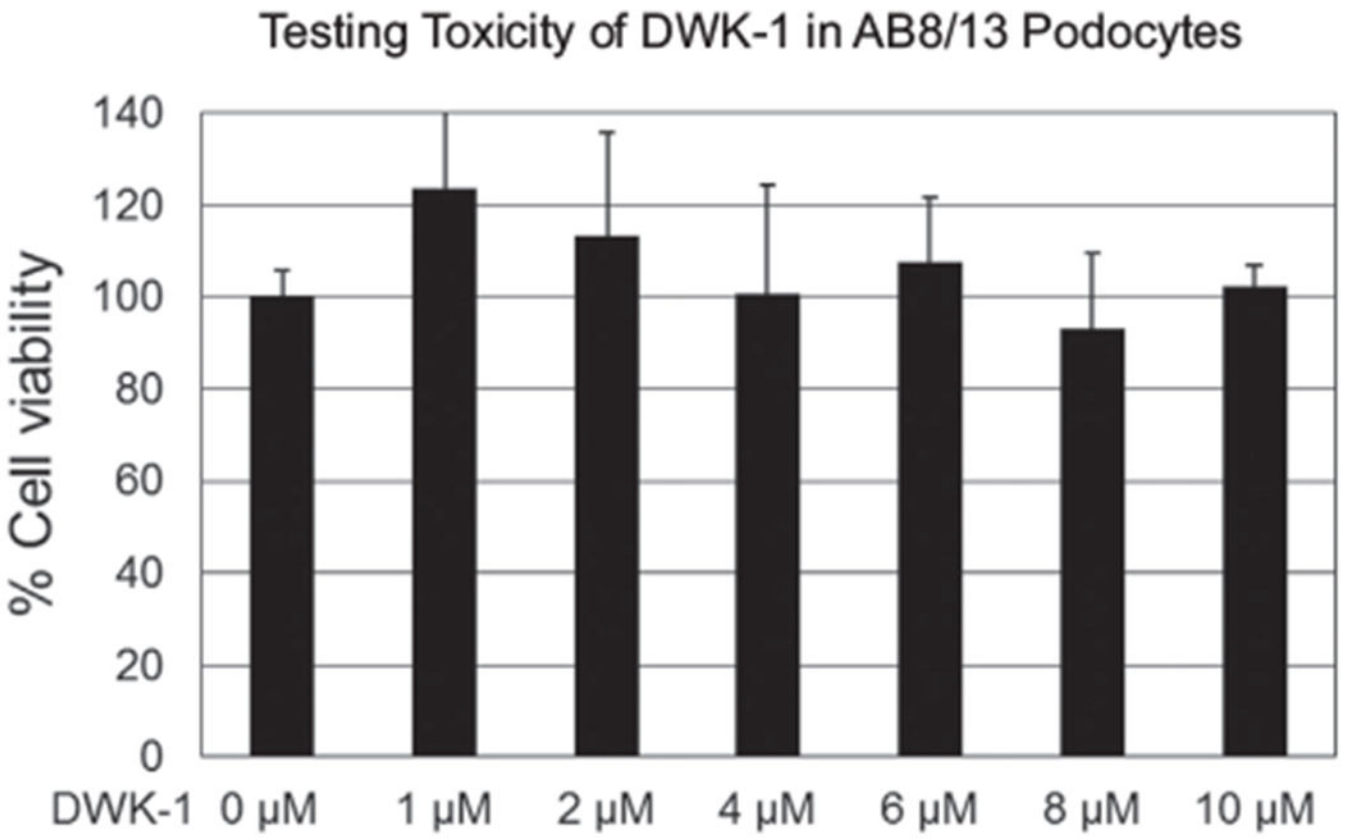

Fig. 2.

Cytotoxicity assay for in vivo-morpholino. Podocytes were exposed in triplicate to DWK-1 at 0–10 uM concentrations and analyzed for cytotoxicity using a Cell cytotoxicity assay kit, Abeam # abll2118 according to the manufacturer protocol. The absorbance intensity was measured at 570 nm and 605 nm using a microplate reader.

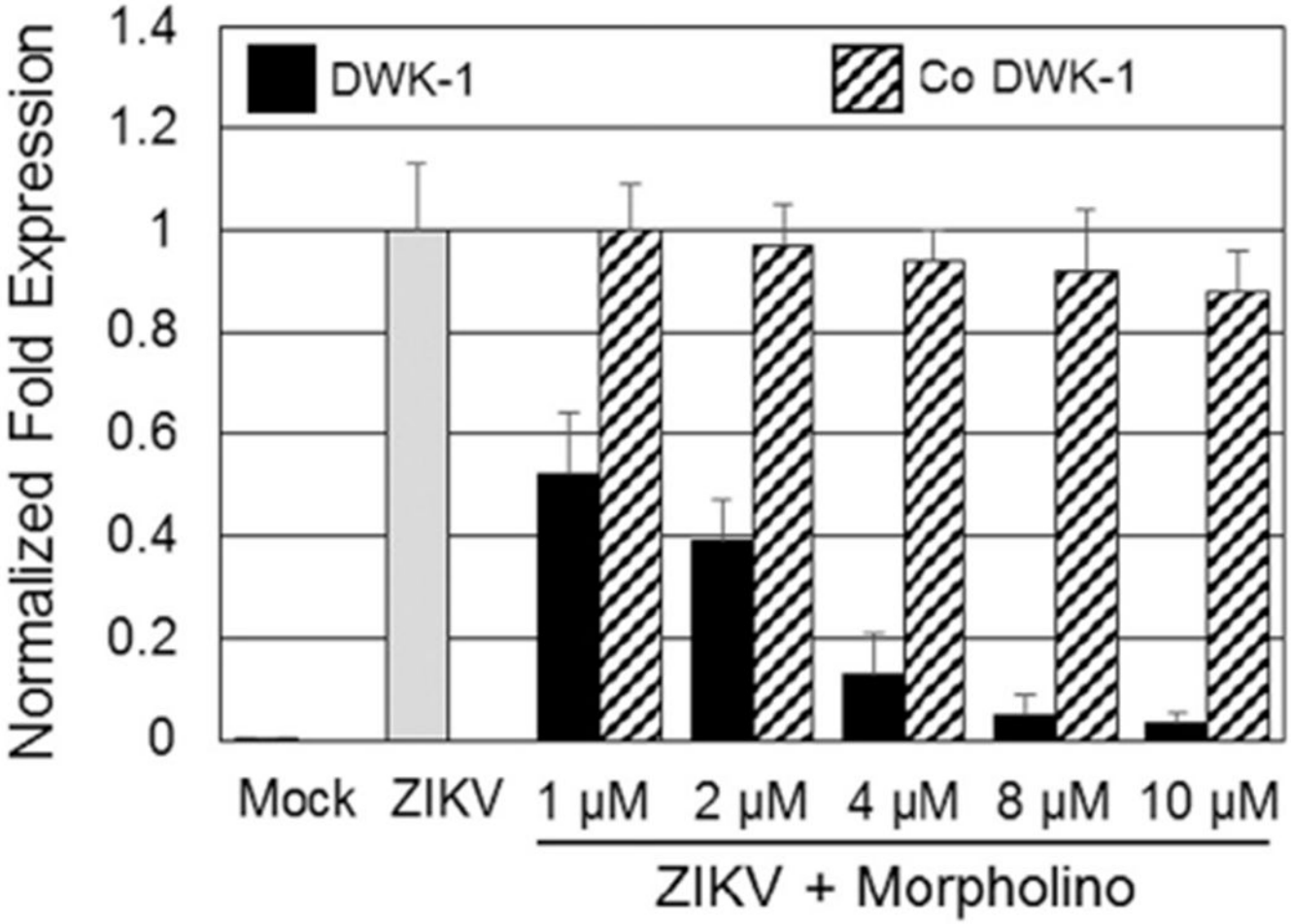

Fig. 3.

Dose-dependent effect of DWK-1 and Co DWK-1 on the accumulation of intracellular ZIKV RNA in infected human podocytes. Podocytes were pretreated for 24 h with the indicated doses of DWK-1 or Co DWK-1, rinsed and infected with ZIKV at MOI of 0.1 in the absence of morpholinos. Total RNA was isolated from the mock infected and ZIKV-infected cells at 72 h p.i. Expression of ZIKV RNA was determined by qRT-PCR and normalized to GAPDH mRNA expression. ZIKV infections were performed in triplicate. Values represent mean ± SD of 3 independent samples. *P < 0.001. ND, not detected.

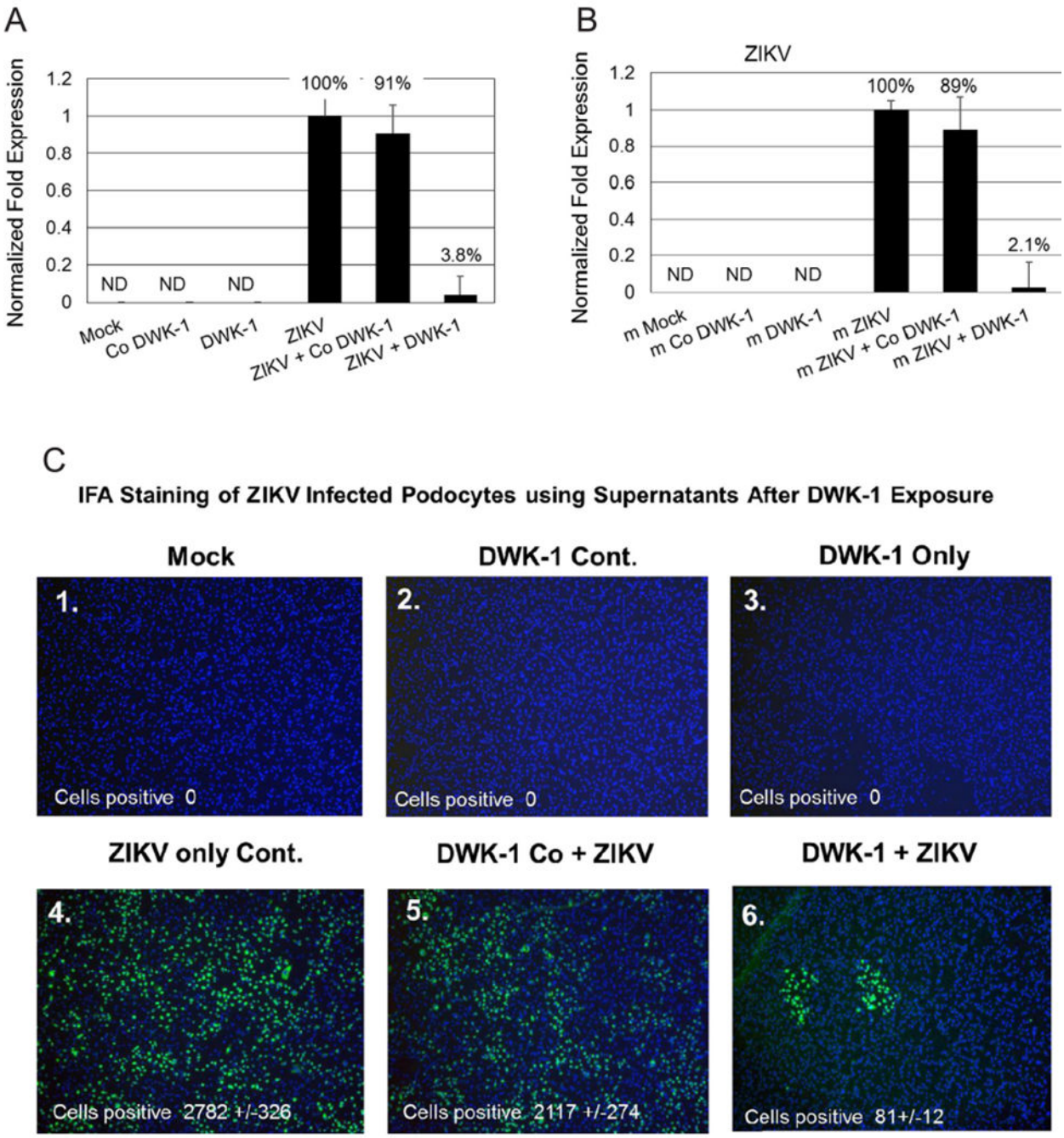

Fig. 4.

DWK-1 suppression of ZIKV progeny released from infected podocytes. (**4A**) qRT-PCR analysis of ZIKV replication in podocytes cultured under different conditions: 1. mock, 2. control morpholino, 3. DWK-1, 4. ZIKV, 5. control morpholino pretreatment and ZIKV, 6. DWK-1 pretreatment and ZIKV. Relative expression of intracellular ZIKV RNA was normalized to GAPDH mRNA. Values represent mean ± SD of 3 independent samples. *P < 0.001. ND, not detected. (**4B**) qRT-PCR analysis of ZIKV progeny released from podocytes cultured under different conditions: 1. mock, 2. control morpholino, 3. DWK-1, 4. ZIKV, 5.

control morpholino pretreatment and ZIKV, 6. DWK-1 pretreatment and ZIKV. Relative expression of intracellular ZIKV RNA was normalized to GAPDH mRNA. Values represent mean ± SD of 3 independent samples. *P < 0.001. ND, not detected. (**4C**). ZIKV progeny released from infected podocytes by fluorescent focus infectivity assay using the 4 G-2 antibody specific to the E protein of ZIKV. (1) mock, (2) control morpholino, (3) DWK-1, (4) ZIKV, (5) control morpholino pretreatment and ZIKV, (6) DWK-1 pretreatment and ZIKV. All cells were stained with the 4 G-2 antibody conjugated FITC and counterstained with DAPI to stain the nuclei. Cells were counted by fluorescent microscopy. Fluorescent images were taken on a Nikon TE2000S microscope mounted with a CCD camera at 200 × magnification. Nuclei (blue) were stained with DAPI.

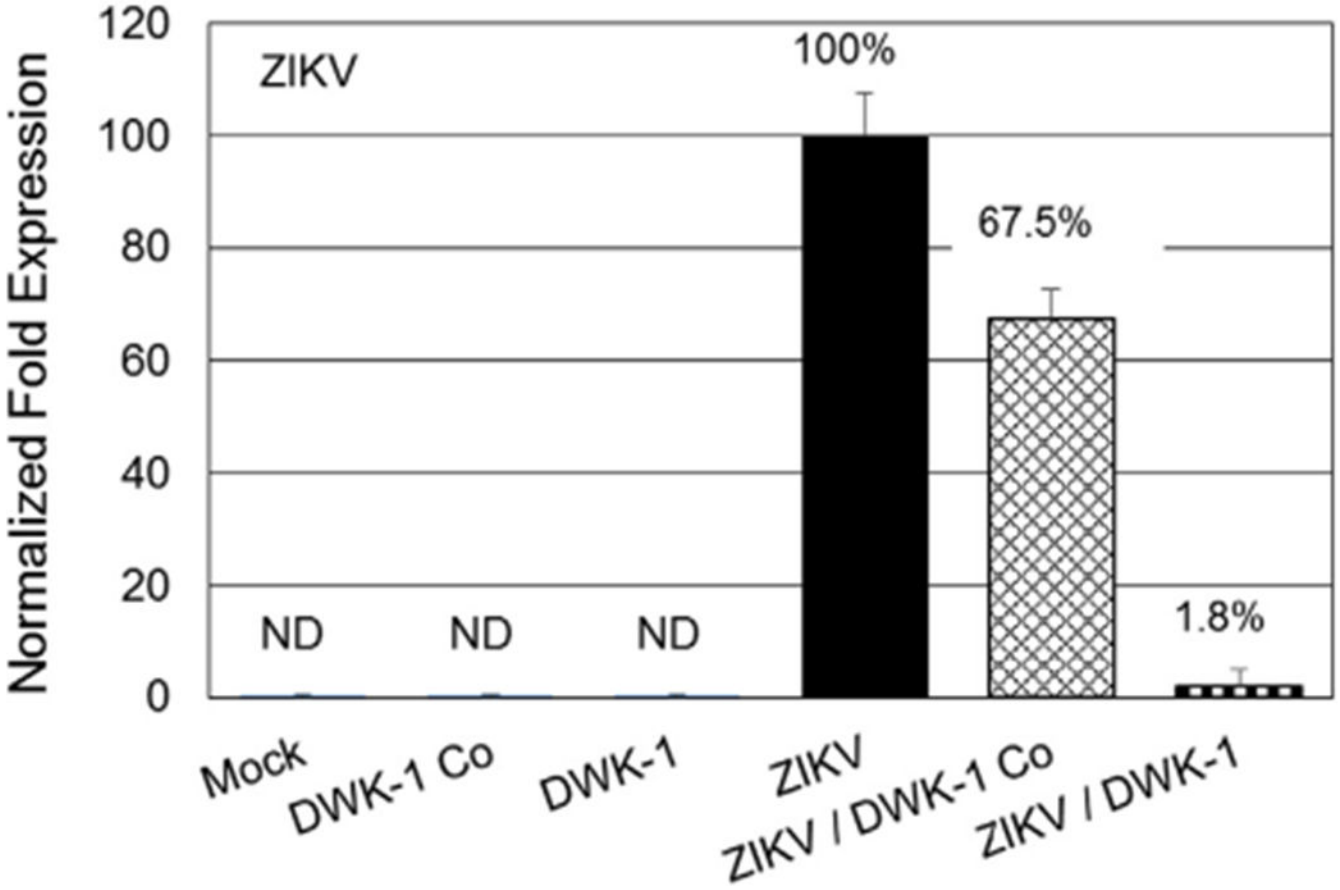

Fig. 5.

DWK-1 inhibition of ZIKV replication in primary human retinal endothelial cells. DWK-1 inhibition of ZIKV transcription in primary human retinal endothelial cells by qRT-PCR. ZIKV RNA accumulation in primary human retinal endothelial cells cultured under different conditions: 1. mock, 2. control morpholino, 3. DWK-1, 4. ZIKV, 5. control morpholino pretreatment and ZIKV, 6. DWK-1 pretreatment and ZIKV. Relative expression of intracellular ZIKV RNA was normalized to GAPDH mRNA. Values represent mean ± SD of 3 independent samples. *P < 0.001. ND, not detected.

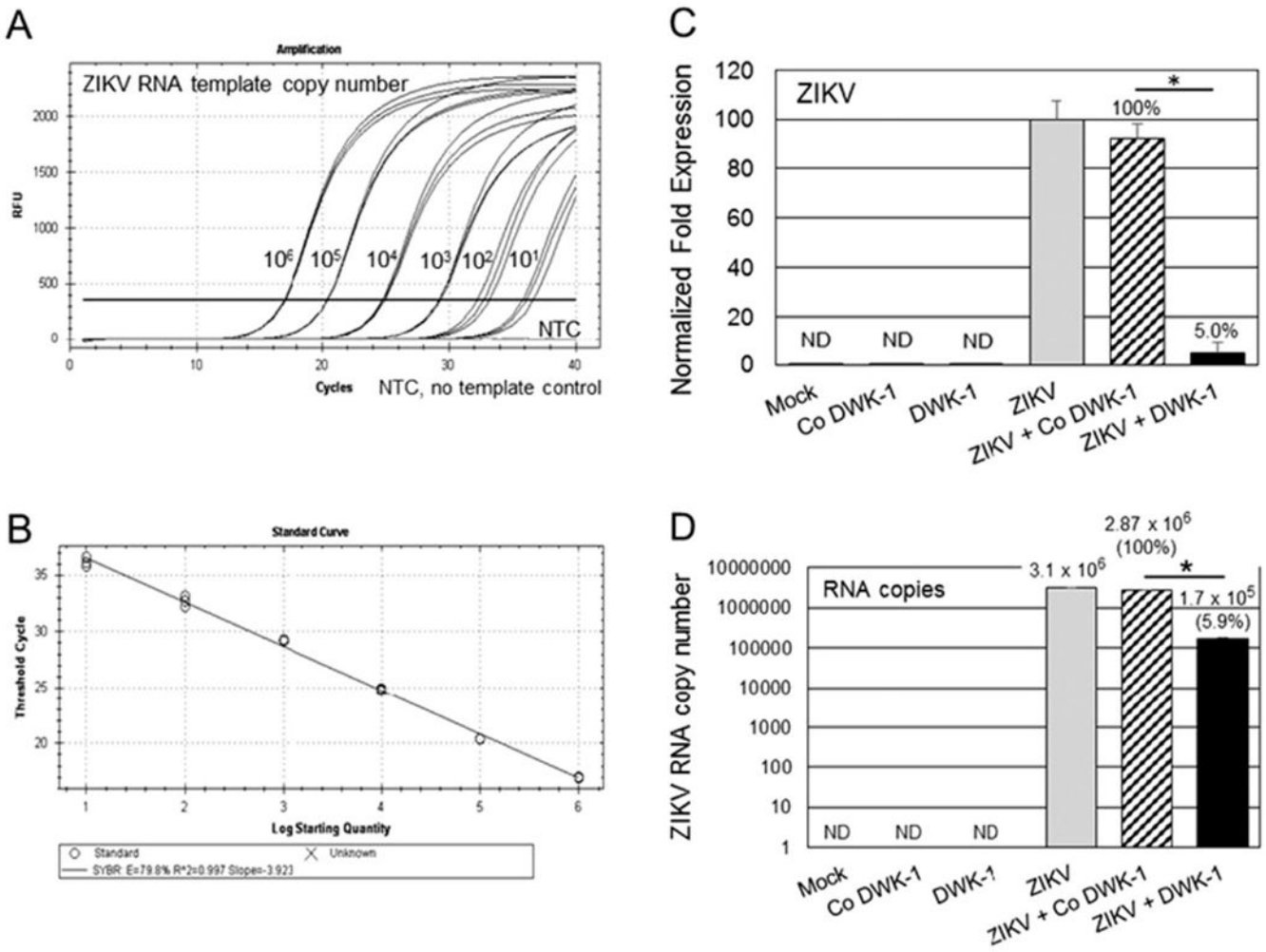

Fig. 6.

DWK-1 reduces ZIKV RNA genome copy number in infected podocytes. (**A**) Ten-fold dilutions of synthetic ZIKV RNA (VR-3252 SD, 10^6 to 10 copies) were amplified by qRT-PCR using ZIKV specific primers. Amplification curves are shown. NTC, no template control. (**B**) The regression line was established by plotting the threshold cycles (C_T) values against the copy number of synthetic RNA. The coefficient of determination R^2 was 0.997 and slope was − 3.923. (**C**) Total cellular RNA isolated from mock, ZIKV infected cells, cells pretreated for 24 h with 10 μM DWK-1 or Co DWK-1 alone, or cells pretreated with morpholinos and infected with ZIKV for 48 h was analyzed by qRT-PCR for the expression of ZIKV and GAPDH RNA. Relative expression of intracellular ZIKV RNA was normalized to GAPDH mRNA. Values represent mean ± SD of 3 independent samples. *P < 0.001. (**D**) Quantitation of ZIKV genome copy number in total intracellular RNA prepared as described in (C) shows 94.1% reduction in ZIKV copy number in infected cells pretreated with DWK-1. Values represent mean ± SD of 3 independent samples. *P < 0.001 ND, not detected.

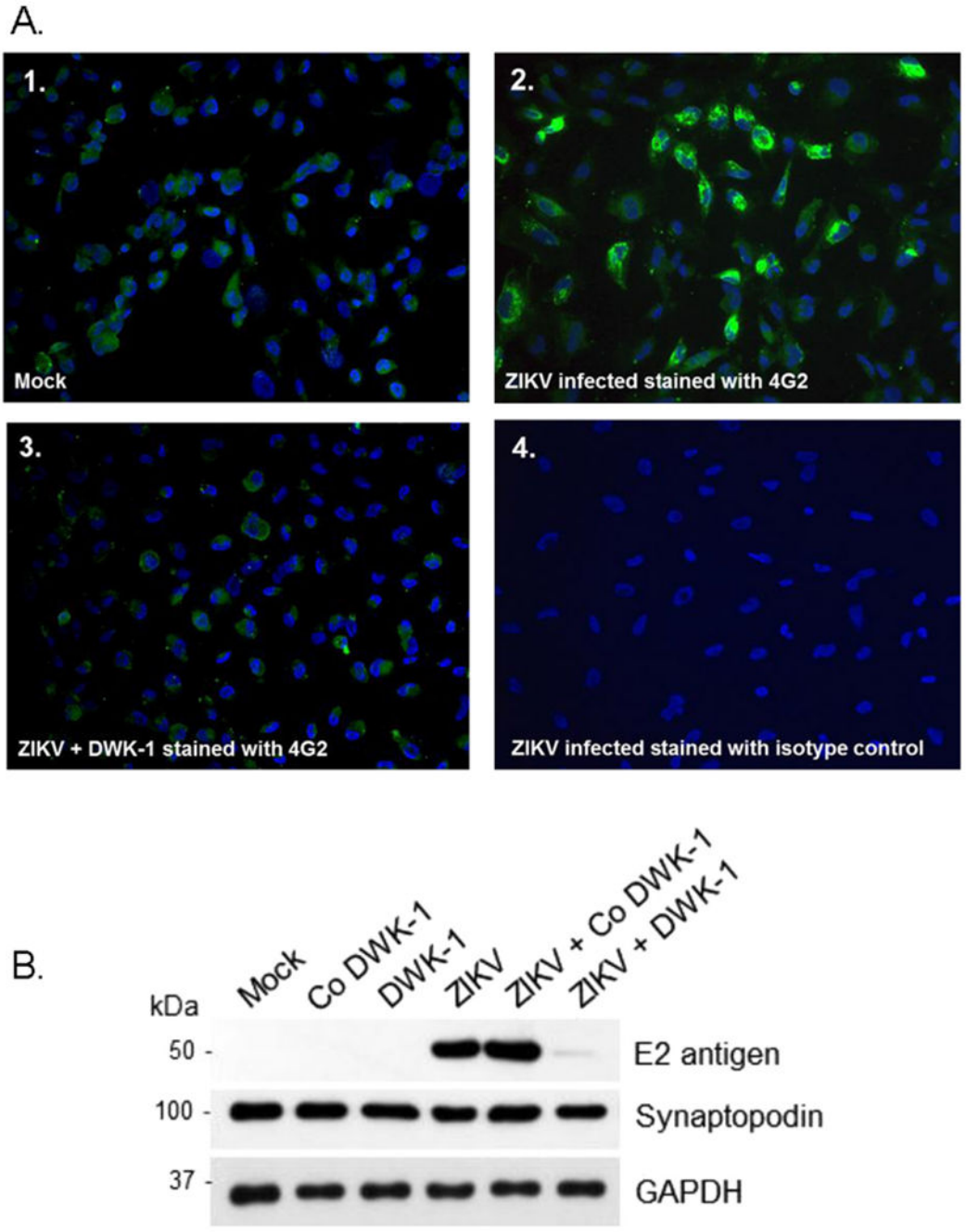

Fig. 7.

A. Immunostaining of ZIKV infected podocytes after treatment with DWK-1. Immunofluorescent staining of ZIKV infected podocytes using the 4G-2 antibody specific to the E protein of ZIKV. (**1**) Mock infected podocytes stained with 4G-2 antibody, (**2**) Podocytes infected with wildtype ZIKV for 72 h and stained with the 4G-2 antibody, (**3**) Podocytes pretreated with DWK-1 for 24 h, rinsed and infected with ZIKV for 72 h were stained with the 4G-2 antibody. (**4**) Isotype control for the 4G-2 antibody. Fluorescent images were taken on a Nikon TE2000S microscope mounted with a CCD camera at 200 ×

magnification. Nuclei (blue) were stained with DAPI. B. *DWK-1 inhibits expression of E protein in ZIKV-infected podocytes*. Western blot analysis of protein lysates from uninfected and ZIKV infected podocytes. Control protein lysates were prepared from mock infected podocytes and podocytes pretreated for 24 h with 10 μM DWK-1 or Co DWK-1, rinsed and cultured for additional 72 h without added morpholinos. Untreated podocytes or cells pretreated for 24 h with DWK-1 or Co DWK-1 were subsequently infected with ZIKV and protein lysates were prepared 72 h after ZIKV infection. The ZIKV expression of the E protein (E2 antigen) is shown in the top panel. The middle panel shows the podocyte biomarker Synaptopodin and the bottom panel shows GAPDH as a loading control.

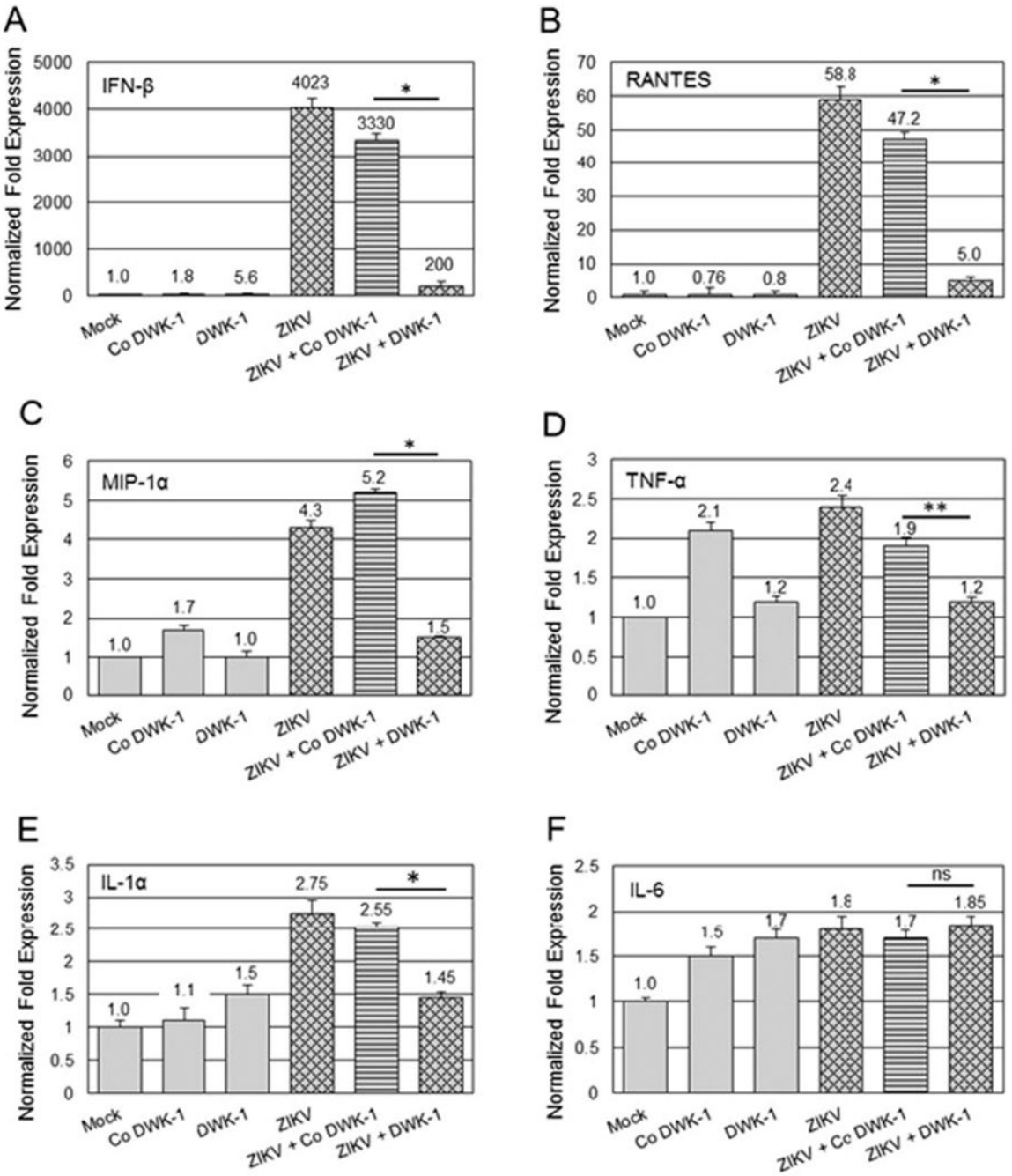

Fig. 8.

DWK-1 inhibits ZIKV-induced proinflammatory cytokine gene expression. Podocytes were pretreated for 24 h with 10 μM DWK-1 or Co DWK-1 and infected with ZIKV at MOI 0.1. Mock infected cells and cells treated only with DWK-1 or Co DWK-1 were included as controls. Total RNA was isolated at 72 h p.i. and indicated cytokine gene expression was quantitated by qRT-PCR and normalized to GAPDH mRNA. Results show the effect of DWK-1 and Co DWK-1 on the expression of selected cytokine genes in ZIKV infected podocytes: (**A**) IFN-β, *P < 0.001 (**B**) RANTES, *P < 0.001 (**C**) MIP-1α, *P < 0.005 (**D**)

TNF-α, **P < 0.01 (**E**) IL-lα, *P < 0.01, and (F) IL-6, ns (statistically not significant). Values represent mean ± SD of 3 independent samples. The expression of cytokine genes mRNA in mock infected cells was set as 1.0.